WILEY Global Change Biology

Microbial functional diversity covaries with permafrost thaw-induced environmental heterogeneity in tundra soil

Mengting M. Yuan[1,2] | Jin Zhang[1,2] | Kai Xue[1,2,3] | Liyou Wu[1,2] | Ye Deng[1,2,4] |
Jie Deng[1,2,5] | Lauren Hale[1,2] | Xishu Zhou[1,2,6] | Zhili He[1,2] | Yunfeng Yang[7] |
Joy D. Van Nostrand[1,2] | Edward A. G. Schuur[8] | Konstantinos T. Konstantinidis[9] |
Christopher R. Penton[10] | James R. Cole[11] | James M. Tiedje[11] | Yiqi Luo[2] |
Jizhong Zhou[1,2,7,12,13]

[1]Institute for Environmental Genomics, University of Oklahoma, Norman, OK, USA

[2]Department of Microbiology and Plant Biology, University of Oklahoma, Norman, OK, USA

[3]University of Chinese Academy of Sciences, Beijing, China

[4]Research Center for Eco-Environmental Sciences, Chinese Academy of Sciences, Beijing, China

[5]School of Ecological and Environmental Sciences, East China Normal University, Shanghai, China

[6]School of Minerals Processing and Bioengineering, Central South University, Changsha, China

[7]School of Environment, Tsinghua University, Beijing, China

[8]Center for Ecosystem Sciences and Society, Department of Biological Sciences, Northern Arizona University, Flagstaff, AZ, USA

[9]School of Civil and Environmental Engineering, School of Biological Sciences, Georgia Institute of Technology, Atlanta, GA, USA

[10]College of Integrative Sciences and Arts, Arizona State University, Mesa, AZ, USA

[11]Center for Microbial Ecology, Michigan State University, East Lansing, MI, USA

[12]School of Civil Engineering and Environmental Sciences, University of Oklahoma, Norman, OK, USA

[13]Earth and Environmental Sciences, Lawrence Berkeley National Laboratory, Berkeley, CA, USA

Correspondence
Jizhong Zhou, Department of Microbiology and Plant Biology, Institute for Environmental Genomics (IEG), University of Oklahoma, Norman, OK, USA.
Email: jzhou@ou.edu

Funding information
US Department of Energy, Office of Science, Genomic Science Program, Grant/Award Number: DE-SC0004601, DE-SC0010715; NSF LTER Program; Office of the Vice President for Research at the University of Oklahoma; Collaborative Innovation Center for Regional Environmental Quality; Office of Biological and Environmental Research; Terrestrial Ecosystem Science (TES) Program, Grant/Award Number: DE-SC0006982, DE-SC0014085; National Parks Inventory and Monitoring Program; National Science Foundation Bonanza Creek LTER Program, Grant/Award Number: 1026415

Abstract

Permafrost soil in high latitude tundra is one of the largest terrestrial carbon (C) stocks and is highly sensitive to climate warming. Understanding microbial responses to warming-induced environmental changes is critical to evaluating their influences on soil biogeochemical cycles. In this study, a functional gene array (i.e., GEOCHIP 4.2) was used to analyze the functional capacities of soil microbial communities collected from a naturally degrading permafrost region in Central Alaska. Varied thaw history was reported to be the main driver of soil and plant differences across a gradient of minimally, moderately, and extensively thawed sites. Compared with the minimally thawed site, the number of detected functional gene probes across the 15–65 cm depth profile at the moderately and extensively thawed sites decreased by 25% and 5%, while the community functional gene β-diversity increased by 34% and 45%, respectively, revealing decreased functional gene richness but increased community heterogeneity along the thaw progression. Particularly, the moderately thawed site contained microbial communities with the highest abundances of many genes involved in prokaryotic C degradation, ammonification, and nitrification processes, but lower abundances of fungal C decomposition and anaerobic-related genes.

Significant correlations were observed between functional gene abundance and vascular plant primary productivity, suggesting that plant growth and species composition could be co-evolving traits together with microbial community composition. Altogether, this study reveals the complex responses of microbial functional potentials to thaw-related soil and plant changes and provides information on potential microbially mediated biogeochemical cycles in tundra ecosystems.

1 | INTRODUCTION

Northern permafrost regions have accumulated approximately 1,700 Pg C, representing about 50% of global belowground C (Ciais et al., 2013; Tarnocai et al., 2009). Most of this C has been preserved frozen for thousands of years (Schuur et al., 2008). Nonetheless, climate warming has caused substantial regional permafrost thaw (Jorgenson, Racine, Walters, & Osterkamp, 2001; Lawrence & Slater, 2005; Osterkamp, 2007; Romanovsky, Smith, & Christiansen, 2010), thickened the seasonally melted active layer and created more unfrozen taliks in recent decades (Chapin et al., 2005; Euskirchen et al., 2006; Natali et al., 2011). Thus, this permafrost C pool can potentially be converted into a significant C source to the atmosphere by the end of this century through the release of large amounts of greenhouse gases, primarily carbon dioxide and methane (CO_2 and CH_4), that serve as a positive feedback to climate warming (Abbott et al., 2016; Schuur et al., 2013, 2015).

As soil microorganisms are pivotal mediators of the C cycle in terrestrial ecosystems, monitoring microbial responses to thaw is crucial for predicting C sequestration in permafrost regions. They play a fundamental role in soil organic C decomposition and impact plant C fixation through nutrient exchange with aboveground ecosystems (Van Der Heijden, Bardgett, & Van Straalen, 2008). Recently, a few studies have provided evidence of tundra microbial functional potential shifts in response to warming or fire (Taş et al., 2014; Xue, Yuan, Shi, et al., 2016), which may alter C allocation and cycling. Lipson et al. (2015) showed that soil redox conditions were the dominant force in shaping microbial communities in a polygonized tundra landscape, and that higher redox potentials allowed for greater microbial diversity. Two independent studies by Mackelprang et al. (2011) and Coolen and Orsi (2015) both incubated permafrost soil and discovered rapid shifts in microbial functional genes and transcriptomes within 2 weeks upon thaw. Thus, temperature and redox conditions both play a role in tundra soil dynamics, and may be critical in shaping microbial community composition, function, and ultimately, tundra C cycling upon permafrost thaw. Yet observations matching the time scale of long-term and naturally occurring permafrost thaw is still lacking, coupled with a limited understanding of detailed influences of such environmental perturbation on microbial functional genes (Mackelprang, Saleska, Jacobsen, Jansson, & Taş, 2016).

In the past two decades, a series of studies have characterized an acidic tundra study site near Eight Mile Lake (EML) in Healy, Alaska. Three locations in this site were identified as minimal (Mi), moderate (Mo), and extensive (Ex) thaw based on both historical records and environmental observations (Osterkamp, 2007; Osterkamp & Romanovsky, 1999; Schuur et al., 2009). The Mi site represents the early stage of permafrost degradation in tussock tundra. The Mo site has documented thawing and ground subsidence since 1985. Thawing at the Ex site, where substantial ground subsidence and periodical thermokarst formation were observed, is estimated to have started in the 1950s (Schuur et al., 2009). The differences in thaw extent among the three sites are caused by spatially randomized positive feedbacks among temperature alteration, ground subsidence, hydrological movements, and further thawing. Thus, the divergence in plant communities and soil properties observed presently are mainly due to permafrost thaw (Schuur et al., 2009). This site provided a unique opportunity to study the effects of decadal-long permafrost thaw on the ecosystem. Plant community succession in response to thaw exhibited larger plant biomass and aboveground net primary productivity (ANPP), as well as the replacement of dominant graminoid species with increased abundances of deciduous and evergreen shrubs (Schuur, Crummer, Vogel, & Mack, 2007). Despite the greater C fixation by plants, radiocarbon analysis suggested that this area was transformed to a C source from a historical C sink due to recent warming-induced increases in respiration (Hicks Pries, Schuur, & Crummer, 2012, 2013; Schuur et al., 2009). Although the C storage was similar among sites, the Ex thaw site showed a two- to three-fold increase in old C loss, and old C comprised 8% more of the ecosystem respiration, compared with that of the Mi thaw site (Schuur et al., 2009).

Recently, amplicon sequencing of the 16S rRNA genes and *nifH* genes revealed that the microbial phylogeny as well as the *nifH* harboring communities in the EML site soils were distinct along soil depth profiles, and responded to thaw differently in varied layers corresponding to thaw depth and water table (Deng et al., 2015; Penton et al., 2016). Here, we specifically focused on detecting and analyzing functional gene abundances in these soils using a functional gene array, GEOCHIP 4.2, to address the following questions: (i) How do natural permafrost thaw and varying thaw histories impact microbial community functional gene composition and abundance? and (ii) What are the environmental factors influencing these

compositional and abundance-based changes? This study provides detailed microbial functional gene responses due to the influence of long-term and naturally occurring permafrost thaw, which serve as a reference for a mechanistic understanding of the future C balance of tussock tundra.

2 | MATERIALS AND METHODS

2.1 | Site and sample description

The thaw gradient sites are located on a moist acidic tundra in the discontinuous permafrost region (63°52′42″N, 149°15′12″W, 660–700 m elevation) (Lee, Schuur, & Vogel, 2010; Schuur et al., 2009; Trucco et al., 2012; Vogel, Schuur, Trucco, & Lee, 2009). Distances between Ex and Mo, Mo and Mi, and Ex and Mi sites were about 150 m, 380 m, and 530 m, respectively. The thaw depth, or the thickness of unfrozen surface soil, was measured every 1–10 days from May to September 2004 (corresponding to the year when microbial samples were taken) and at the time of soil sampling. A metal rod was inserted into the ground until the frozen layer was reached, and the length of insertion was recorded as thaw depth. The active layer depth, referring to the length from the deepest thawed soil in the summer time to the ground surface, was the largest thaw depth recorded during the growing season (Schuur et al., 2009). Soil temperature was recorded every 2 hr at depths of 10, 20, 30, and 40 cm by a copper/constantan thermocouple (Schuur et al., 2009). The ground surface microtopography for each site was estimated as the standard deviation of local-scale elevation measurements, with the effect of overall hillslope statistically removed. The microtopography is a measure of ground surface unevenness caused by thermokarst depressions, a topological sign of permafrost thaw that reforms the tundra landscape (Osterkamp et al., 2009).

Replicate sampling cores in each site were located within 50 m of one another. Soil sampling for physiochemical and microbial analyses was described previously (Hicks Pries et al., 2012). Briefly, six soil cores were collected at each of the three thawing sites at the beginning of the growing season (May 2004). Half of the 18 cores reached permafrost, which ranged in depth from 50–130 cm below surface. All cores avoided tussocks. Layers of each soil column were separated by depth using the following seven categories; 0–15, 15–25, 25–35, 35–45, 45–55, 55–65 cm, and below 65 cm. In some cases, cores did not extend into the full profile. Altogether, 107 samples were obtained, 32 from Mi, 26 from Mo, and 39 from Ex sites. Among them, 93 samples were from active layers and 14 from permafrost layers. The number of samples acquired for each depth was shown in Table S1. At the time of sampling (spring), 23 fractions were already seasonally thawed while 84 remained frozen. Samples were transferred frozen from the field to the laboratory where they were stored at −20°C until further processing. Soil moisture was calculated as the percentage weight loss after drying the samples at 60°C. The bulk density was determined by the ratio of soil dry weight and bulk volume determined at the time of sampling (Hicks Pries et al., 2012). Dried samples were used to analyze soil nitrogen (N), C content, and $\delta^{15}N$ and $\delta^{13}C$ ratios on a Costech (ECS4010) Elemental Analyzer coupled with an isotope ratio mass spectrometer (Hicks Pries et al., 2012).

2.2 | DNA extraction

Genomic DNA was extracted and purified from 5 g of soil for each sample using a PowerMax Soil DNA Isolation Kit (MO BIO Laboratories, Inc., Carlsbad, CA, USA). The concentration of DNA was quantified using Quant-iT PicoGreen dsDNA Assay Kit (Thermo Fisher Scientific, Waltham, MA, USA) on an FLUOstar OPTIMA fluorescence plate reader (BMG LabTech, Jena, Germany). DNA quality was checked on a NanoDrop ND-1000 Spectrophotometer (NanoDrop Technologies Inc., now NanoDrop Products by Thermo Fisher Scientific). The spectrometry absorbance ratios at 260/280 nm were between 1.7 and 2.2, and the 260/230 nm ratios were >1.8.

2.3 | Labeling and GEOCHIP hybridization

GEOCHIP version 4.2 is a NIMBLEGEN format comprehensive gene array containing 107,950 different 50-mer probes and covering 790 microbial functional genes that encode enzymes for biochemical reactions, including C, N, phosphorus, sulfur cycling, and seven other major categories (Tu et al., 2014). From each sample, 1 μg DNA was fluorescently labeled for hybridization. The labeling, hybridization, and scanning were processed following the protocols previously described (Xue, Yuan, Shi, et al., 2016).

2.4 | GEOCHIP data preprocessing

Data normalization was completed on a web-based pipeline (http://ieg.ou.edu/microarray/) as follows. First, the raw probe signals, calculated based on the average pixel intensity of each probe, were adjusted based on control dye intensity and sample set total intensity. Second, signals were filtered by removing the spots with a signal-to-noise ratio <2, and the spots with signal intensity <2 times background. Third, probes that generated positive signals in <10% of the samples from a given thaw site (all replicates from within each field site and along the depth profile) were considered low abundance genes and removed from that site for downstream analyses. We identified low abundance genes on a site basis instead of globally to retain functional gene probes unique to one site. Fourth, the probe signals were then normalized to represent relative abundance of genes in each sample. Unless otherwise specified, all gene abundance data reported in this manuscript represent relative abundance estimations based on the normalized signal intensities of probes targeting said gene. A subset of 70 samples, 23 from Mi, 24 from Mo, and 23 from Ex sites, from depth ranges of 15–65 cm that exhibited a greater variation between sites with regard to functional genes detected with GeoChip were the most responsive to thaw. Detailed analyses on these layers were performed separately where indicated. The raw and normalized data can be accessed through the series accession number GSE97107 in the Gene Expression Omnibus (GEO) database.

2.5 | Statistical analysis

Normalized GeoChip signals, as well as soil and plant data, were used in the following analyses. (i) Microbial functional gene α-diversity was estimated using positive probe numbers and Shannon-Weiner, Simpson, and Piedou's evenness (J) were calculated (Hill, 1973). The β-diversities of functional genes among sites were compared using the multivariate homogeneity of group dispersion (Anderson, Ellingsen, & Mcardle, 2006), based on the Sørensen index. The relationship between β-diversity and site surface microtopography was determined using Pearson's product moment correlation. (ii) Welsh permutational t-tests were used to compare the diversity indices between each pair of two sites. p values were adjusted based on false discovery rate for the three comparisons. (iii) One-way ANOVAs followed by Fisher's LSD tests were used to test the difference in means among sites for the soil physical-chemical variables, DNA yields, and gene abundances. p values of F tests on gene abundance were corrected among all the detected genes based on false discovery rates, and p values from the LSD test for each individual gene were adjusted using Holm's method. (iv) Repeated measures ANOVAs were carried out to compare soil temperatures among sites. (v) Nonparametric multivariate statistical analyses, including Multiresponse Permutation Procedures (MRPP) (Van Sickle, 1997), Analysis of Similarity (ANOSIM) (Clarke, 1993), and Permutational Multivariate Analysis of Variance Using Distance Matrices (Adonis) (Anderson, 2001), were used to determine the dissimilarity of microbial functional gene profiles among sites and/or depth profiles. Pairwise distances among samples were calculated based on Bray–Curtis indices. When applicable, observations are permuted within the strata of hybridization slide (11–12 samples per slide) to eliminate potential slide effects; (vi) Mantel tests and canonical correspondence analyses (CCA) (Legendre & Legendre, 2012) were performed to test correlations between microbial functional composition and soil and plant variables. One set of plant properties was used for each site when performing correlation analysis, which sufficed given the low within-site plant variability compared to variability among sites. Samples containing missing soil data were removed from Mantel tests or CCA model construction. The soil and plant variable set in the CCA model was determined by forward selection. All statistical analyses were performed with R program version 3.0.1 (R Core Team, 2014) using the packages VEGAN (Oksanen et al., 2013) and AGRICOLAE (De Mendiburu, 2014).

3 | RESULTS

3.1 | Impacts of thaw on microbial functional gene composition and structure

The highest DNA yield originated from 25–35 cm while the lowest was isolated from the top 15 cm and below 65 cm. No significant differences in DNA yield among sites were observed (Fig. S1). Microbial functional gene composition was distinct among sites, specifically in the active layer (p = .001), but only marginally significant (p < .1) with depth (Table S1). Comparing the communities among sites within depth fractions resulted in detectable differences only in the middle layers (15–65 cm) rather than surface and deep soils (Table S1). Notably, this middle fraction of soil represents depths that were frozen at the time of sampling, but which are still portions of the active layer (Fig. S2).

Functional gene composition from the 70 subsurface samples significantly (p < .05) differed among sites (Table 1), indicating a substantial impact of thaw on these communities. More unique probes in the Mi site (7.07%, 3298 probes) were detected than in the Ex site (1.50%, 697 probes) and the Mo site (0.11%, 52 probes, Figure 1a), rendering the functional gene α-diversity the highest in the Mi site, followed by the Ex site, and lowest at Mo (p < .05, Table S2). Evenness exhibited an opposite trend, highest in Mo and lowest in Mi (p < .05, Table S2). The site-unique functional gene probes were analyzed by the functional categories they belonged to, and compared with the portion of probes designed on GeoChip (Figure 1b). The functional category composition for these site-unique probes was similar in Mi and Ex sites, but different from the Mo site. A smaller portion (4%) of the Mo site-unique probes belonged to the C cycling category, compared with Mi (12%) and Ex (12%) sites. Larger portions of Mo site-unique probes belonged to N (17%) and sulfur (S) (8%) categories, compared with the other two sites (both 9% for N, and 5% and 3% for S in Mi and Ex sites). Despite the similar physical distances among replicate cores within site and similar sampling depth profiles, the functional gene β-diversity increased at both the Mo and Ex sites, in contrast with the Mi site (Figure 2a, p < .05), as indicated by the larger average distance from samples to each of their group centroids. The sparseness of microbial functional community composition was strongly correlated ($R^2 = 0.98$, p = .14, n = 3 sites, Figure 2b) with the surface microtopography of the tundra. Together, both the α- and β-diversities of the soil microbial functional genes were affected by thaw extent.

3.2 | Effects of permafrost thaw on the abundances of important functional genes

A total of 34,017 functional gene probes were detected, 49.1% of which showed significantly (p < .05) different abundances among sites (Table S3). These probes belonged to 692 functional genes. Below are the detailed results for selected categories of functional genes that are important in biogeochemical cycles and ecosystem functioning, including those in C cycling, N, phosphorous (P), S, and plant beneficial categories.

3.2.1 | C cycling genes

A total of 3,305 bacterial and archaeal probes, representing 30 genes associated with metabolizing various C compounds, were detected. Twelve of these genes were significantly (p < .05) different in abundance between at least two of the three sites (Figure 3). Eight of these genes (of 12, 67%) had the highest abundance at the Mo site. For fungal communities, 2,052 probes belonging to 51 genes were detected, and 28 of these genes differed (p < .05) in abundance at

least between two sites (Fig. S3). A majority of these genes (23, 82%) exhibited the lowest abundance at the Mo site.

Four C fixation genes, targeted by 1019 probes, were detected across all samples (Fig. S4). Specifically, aclB gene, an indicator for reductive tricarboxylic acid cycle, and the Calvin cycle rubisco gene were at the lowest abundance in the Mo thaw site. The abundance of the pcc gene, involved in the 3-hydroxypropionate/4-hydroxybutyrate cycle, was highest in the Mo thaw site.

Three methane cycling genes were detected (Fig. S4) with 218, 134, and 196 probes showing positive hybridization signals in the Mi, Mo, and Ex sites, respectively. The abundances of all three genes, including the methane oxidation genes mmoX and pmoA, and methanogenesis gene mcrA, had the lowest abundance in Mo site ($p < .001$). The mcrA gene exhibited a lower abundance at the Ex site compared with the Mi site, although the two methane oxidation genes did not.

3.2.2 | N cycling genes

Eighteen of the 23 detected N cycling genes significantly ($p < .05$) differed in abundances among the three sites (Fig. S5). Under Ex thaw conditions, the N cycling functional potentials were more similar to the Mi site. While the detected ammonification gene gdh abundances decreased with thaw progression, the ureC gene, responsible for conversion of urea into ammonia, was detected in

the highest abundance at the Mo site. Yet, probes targeting nifH genes, involved in N fixation, another ammonium-producing pathway, showed the lowest abundances at the Mo thaw site. The napA gene, involved in nitrate reduction to nitrite, was also lowest in abundance at Mo site. For the ammonia oxidizing gene amoA, 112 detected probes belonged to archaea, and 417 belonged to bacteria. There were greater abundances of bacterial and source organism–unspecified amoA genes, but lower abundances of archaeal amoA genes in the Mo and the Ex site compared with the Mi site. The abundances of all eight detected denitrification genes were impacted by thaw. Except for narG (involved in the first step of denitrification, the reduction of nitrate to nitrite) and a fungal gene p450nor, encoding a cytochrome P450 nitric oxide reductase, the six other denitrification genes, including nirK for both denitrifying and nitrifying pathways, norB, nirS, nosZ, and nirZ, all exhibited the lowest abundances at the Mo site. Assimilatory N reduction genes nirA, nitrate reductase, and nir showed the highest abundance in the Mo site. Overall, microbial functional potentials for organic N ammonification, ammonia oxidation, and assimilatory processes were higher, while N fixation, denitrification, and N mineralization potentials were lower at the Mi site.

3.2.3 | Other functional categories

GeoChip detected abundance differences in genes among the three sites in many other functional categories, and the numbers and portions of those probes are summarized in Table S3. All of the S assimilation (ATP sulfurylase, PAPS reductase, and sulfate transporter) and sulfite reduction (dsrA/B) genes showed the lowest abundance in the Mo site (Fig. S6). A P utilization gene, ppx, was decreased in both the Mo and Ex thaw sites, compared to the Mi site (Fig. S6). For plant beneficial genes, 12 of the 32 (37.5%) detected had the highest abundances at the Mo site, including genes encoding the enzymes for antibiotic (pcbC, imbA, phzF, and prnB), antioxidant (cat), and hormone (sped and spe) biosynthesis, pathogen resistance (sid), and plant hormone signaling (acdS) (Fig. S7).

3.3 | Linkages between microbial functional potentials and soil and plant properties

A summary of reported plant and soil characteristics is shown in Table 2. Soil temperatures in different depths are presented in

TABLE 1 Nonparametric multivariate dissimilarity tests of functional gene profiles among the three sites, and between any two sites. Distinct functional gene profiles were detected in the three sites. MRPP, multiresponse permutation procedures; Adonis, permutational multivariate analysis of variance using distance matrices; ANOSIM, analysis of similarity. Results presented are based on distance matrices calculated with Bray–Curtis index. Horn, Euclidean, and binomial distances were also used, and generated similar outcomes (all tests significant), thus results not shown. p values <.05 are in bold

	MRPP		Adonis		ANOSIM	
	δ	p	F	p	R	p
Among three sites	0.250	.001	11.136	.001	0.234	.001
Mi vs. Mo	0.234	.001	24.750	.001	0.452	.001
Mi vs. Ex	0.244	.005	5.837	.006	0.109	.006
Mo vs. Ex	0.273	.002	5.195	.003	0.117	.008

FIGURE 1 (a) Unique and shared probe number detected in the three thawing sites and (b) the categories those unique probes belonged to. Category "others" includes genes gyrB, and those of energy processes, bacteria phages, bioleaching, metal resistance, organic remediation, and virulence categories
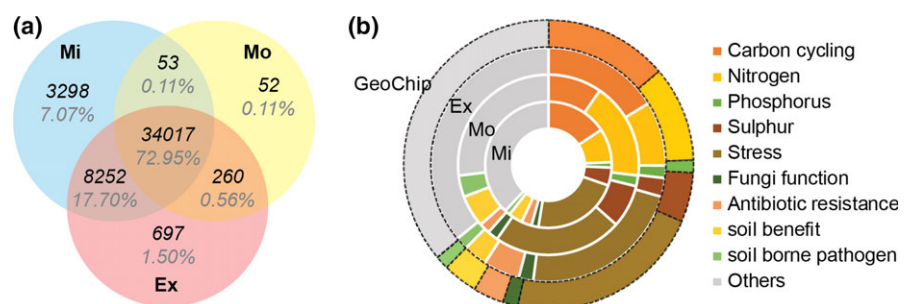
Canonical correspondence analysis (CCA) was performed to establish the linkages of microbial functional gene compositions to plant and soil properties. Variables suggested by forward selection to include in the model consisted of sampling depth, soil moisture, soil C and N content, $\delta^{15}N$, bulk density, vascular plant ANPP, and graminoid ANPP. Mo and Ex site communities were separated from those in the Mi site (p = .005, Figure 4a). The Mi site community functional gene potentials exhibited a negative correlation with vascular plant ANPP, the most influential factor in the model, and a positive correlation with $\delta^{15}N$. The Mo site

functional gene composition was related most to high soil bulk density and graminoid ANPP, and that of the Ex site was positively correlated with soil moisture, as well as C and N content. The model explained 30% of the total variation in microbial functional gene composition.

Variation partitioning analysis (VPA) was performed to identify individual and interactive contributions of different categories of CCA variables to the variances of microbial community structure (Figure 4b). The three categories of variables, plant (vascular plant ANPP and graminoid ANPP), soil physical property (depth,
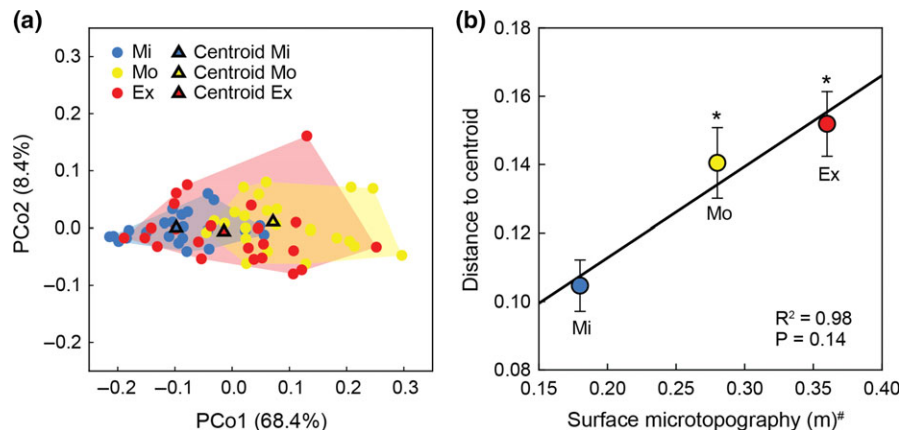

FIGURE 2 (a) The functional gene β-diversity at each site, and (b) its relationship with the surface microtopography. (a) Pairwise distances among samples were calculated using Sørensen index, and processed through multivariate homogeneity of group dispersions procedure to compare the β-diversities among sites. The level of dispersion of samples (represented by circular dots) within each site was measured by the distance of each sample to the site centroid (outlined triangles) in the principle coordinates (PCo) plot. Percentiles in parentheses were the portion of community variation explained by each of the two axes. (b) The means and standard errors of the distances to centroid at each site in (a), in correlation with ground surface microtopography. Surface microtopography was a measure of the unevenness of ground surface. Significant (p < .05, asterisks showed) larger distances to centroid were observed for Mo and Ex sites compared with Mi site by Tukey's test. Linear regression line is shown for n = 3 sites. #Surface microtopography data are adopted from Schuur et al. (2009)
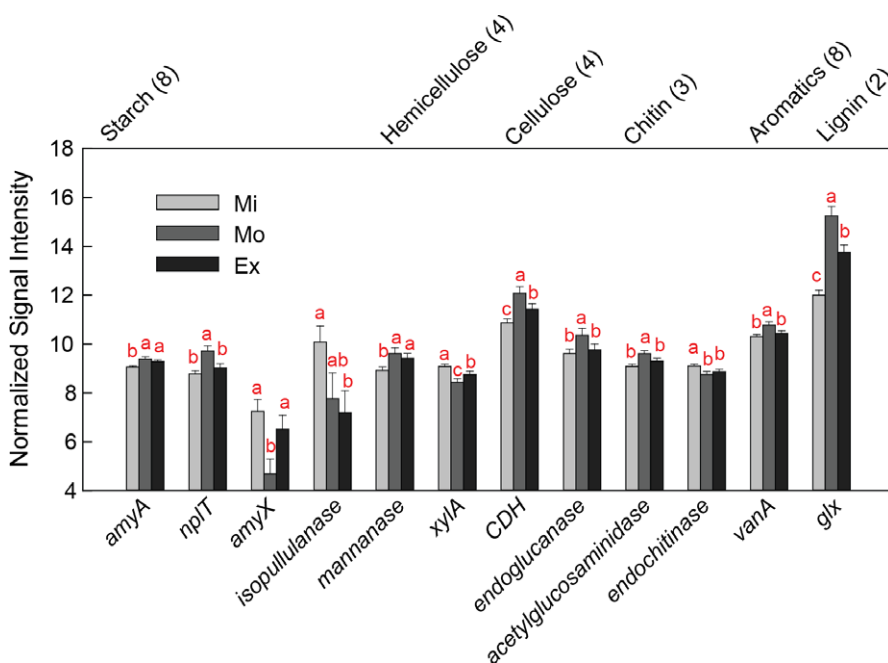

FIGURE 3 Normalized relative abundance of detected C degradation genes derived from bacteria and archaea. Only significantly different abundance among sites was illustrated using bars. The order of genes is organized based on the liability of their targeted C substrate. The numbers in the parenthesis following the gene subcategory (substrate type) indicate the number of total detected genes in that subcategory. In the subcategory of pectin, only one gene is detected (pectinase) and is not significantly different among sites, so it is not shown in the figure. Significant differences in the means are marked by different letters, based on ANOVA model followed by Fisher's LSD test. Full annotation information of the genes is presented in Table S5 [Colour figure can be viewed at wileyonlinelibrary.com]

TABLE 2 Values (mean ± standard error) of soil physical-chemical variables and plant biomass. n = 23, 20, and 16 samples for Mi, Mo, and Ex sites for N, C contents, $\delta^{15}N$, $\delta^{13}C$, and bulk density, and n = 17, 23, 22 for Mi, Mo, and Ex sites for soil moisture, respectively. For plant biomass, n = 12 observations per location. For soil temperature, n = 6 observations for each site. Differences in means among sites were tested using ANOVA followed by LSD test (repeated measures ANOVA was used for daily averaged temperatures data). Different letters denote significant difference in the means. p values <.05 are in bold

Variable	Unit	Mi	Mo	Ex	F	p
Gravimetric water content	%	62.1 ± 4.5	66.1 ± 3.5	69.4 ± 3.4	0.91	.408
Growing season temperature[‡]	°C	3.1 ± 0.3[b]	3.0 ± 0.1[c]	3.4 ± 0.4[a]	979.00	**<.001**
Winter temperature[‡]	°C	−0.1 ± 0.1[b]	−0.1 ± 0.1[c]	0.0 ± 0.1[a]	1148.00	**<.001**
N content[†]	%	1.1 ± 0.1	1.3 ± 0.1	1.2 ± 0.1	1.02	.368
C content[†]	%	26.7 ± 2.7	30.6 ± 2.7	28.9 ± 2.6	0.58	.561
$\delta^{15}N$[†]	‰	0.9 ± 0.1	0.7 ± 0.1	0.9 ± 0.1	1.26	.292
$\delta^{13}C$[†]	‰	−26.2 ± 0.2	−26.4 ± 0.2	−26.3 ± 0.1	0.52	.597
Bulk density[†]	g/cm^3	0.4 ± 0.1	0.4 ± 0.1	0.3 ± 0.1	0.26	.776
ANPP from vascular plant*	g/m^2	187.2 ± 4.1[b]	271.9 ± 9.2[a]	203.6 ± 5.1[ab]	3.96	**.029**
Vascular plant biomass*	g/m^2	248.9 ± 3.6[b]	370.5 ± 10.9[a]	330.9 ± 5.0[ab]	6.13	**.005**
ANPP from non-vascular plant*	g/m^2	23.9 ± 1.7[b]	53.2 ± 4.1[ab]	154.9 ± 13.6[a]	5.77	**.007**
Nonvascular plant biomass*	g/m^2	112.1 ± 4.0[b]	117.3 ± 3.1[ab]	154.8 ± 2.9[a]	3.89	**.030**

*Reanalyzed from Schuur et al. (2007).
[†]Reanalyzed from data presented in Hicks Pries et al. (2012).
[‡]Reanalyzed from Schuur et al. (2009).

moisture, and bulk density), and soil chemistry (N and C contents, $\delta^{15}N$), explained 14%, 6%, and 5% of the total variance, respectively. Interactions between the three groups contributed 5% of the total variance. The majority of the community variations (70%) could not be explained by the plant and soil variables measured.

Mantel tests were used to examine the relationships between microbial functional gene composition and plant and soil variables (Table S4). Microbial functional gene composition was only significantly ($p < .05$) correlated with vascular plant and graminoid biomass and ANPP. Nonvascular plant variables and soil geochemical variables were not correlated with microbial functional gene profiles.
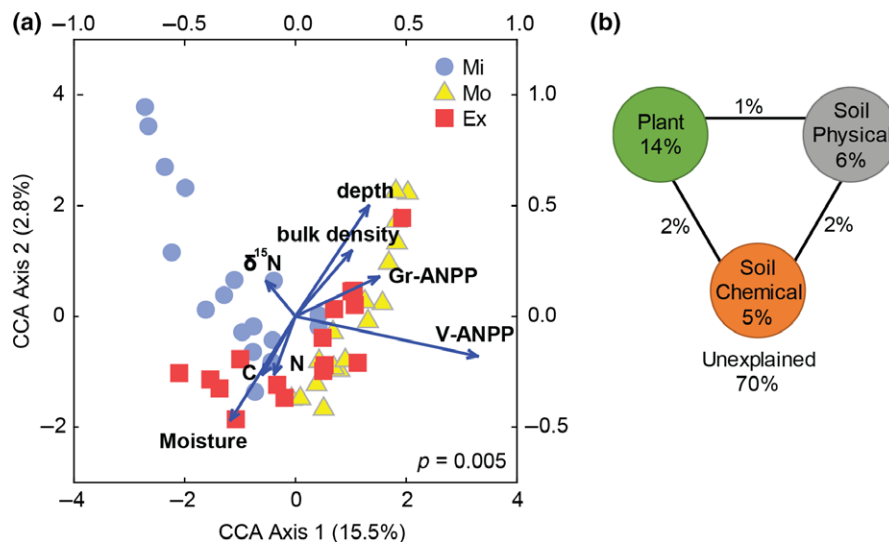

FIGURE 4 (a) Canonical correspondence analysis (CCA) and (b) variation partitioning analysis (VPA) on microbial functional gene profiles and forward selection determined plant and soil variables. A total of 57 sample points (after removing samples having missing soil variable measurements) from the three thawing sites and eight plant and soil geochemical variables were included. Numbers on CCA axis and in VPA diagram show the percentages of explained variations in the microbial functional gene profile. Lower and left axes show scales for microbial functional gene profiles, and the upper and right axes show scales for plant and soil variables. V-ANPP, vascular plant aboveground net primary productivity; Gr-ANPP, graminoid ANPP. In VPA, plant variables include Gr-ANPP and V-ANPP, soil physical properties include moisture, and bulk density, and sampling depth; soil chemical variables include N, C, and $\delta^{15}N$ [Colour figure can be viewed at wileyonlinelibrary.com]

Controlling for the variations caused by depth did not reveal any significant correlations between soil variables and microbial functional gene composition.

4 | DISCUSSION

As one of the most vulnerable terrestrial C pools, decomposition of organic C in thawing permafrost may serve as a positive feedback to global climate change (Schuur & Abbott, 2011), but also difficult to predict owing to the complexity of belowground microbial activities. This study observed the tundra microbial functional potentials in sites exposed to varied intensity of permafrost thaw. We found shifts in microbial functional gene profiles from minimally to extensively thawed sites at 15–65 cm, with lower α-diversity and higher β-diversity at the two more severally thawed sites compared with minimal thaw. This is more or less consistent with previous studies at the same site (Deng et al., 2015; Penton et al., 2016), as well as with other studies which showed thaw-related perturbations affected the tundra microbial communities in laboratory microcosms (Mackelprang et al., 2011; Taş et al., 2014), field experiments (Xue, Yuan, Shi, et al., 2016), and field observations (Lipson et al., 2015). Microbial diversity is expected to increase as permafrost thaws because more substrates become available (Jansson & Taş, 2014), yet field evidence is lacking, possibly due to insufficient survey efforts (e.g., sequencing depth) to detect such difference. Conspicuously, difference in microbial functional gene profile was not observed in the surface (0–15 cm) and permafrost (>65 cm) layers. Passive dispersal of microorganism through air or animal carrier (Martiny et al., 2006) might easily homogenize the species pool in top soils within the area of our study site. While in continuously frozen permafrost, harsh condition caused limited growth and activity (Rivkina et al., 2004) might be the reason of slow microbial succession upon disturbance. The increase in the functional gene β-diversity with thaw is an intriguing finding highlighted by this study. The level of divergence of functional gene potentials from communities within a similar physical distance was strongly correlated with the surface microtopography, a measure of the unevenness of ground surface created by thermokarst depressions (Schuur et al., 2009). This indicated that thaw-induced topographical reformation and thus increased versatility of soil environment may be the primary reason for the increase in the heterogeneity in microbial functional gene compositions.

As thaw progressed, a large portion of detected functional genes that are involved in C, N, and other biogeochemical cycling changed in abundances, most of which were not merely increase or decrease from the least to the most thawed sites, but rather showed extreme values at the moderate thaw. On the other hand, vascular plant biomass and ANPP both peaked at moderate thaw, before shrubs took over graminoids under warmer and extensively thawed conditions (Schuur et al., 2007). Tundra soil is C rich, but with a large portion being slow C (Schuur et al., 2008), whose decomposition was primarily stimulated by inputs of fresh and labile C, mainly from succeeding plants (Grogan, Illeris, Michelsen, & Jonasson, 2001). Both the composition and abundance of plant species can affect the belowground microbial assemblages (Bais, Weir, Perry, Gilroy, & Vivanco, 2006). At moderate thaw, the most abundant C degrading genes harbored by bacteria and archaea vs. the least abundance of those genes carried by fungi might reflect variations in the amount of litter- and root exudate-derived C substrates among sites. Grass dominance and larger plant biomass at moderate thaw might provide more high-quality litter as well as root exudates for bacteria. In contrast, shrub dominance at the extensively thawed site possibly led to low-quality, standing litter (Gavazov, 2010; Hobbie, 1996), thus supporting a higher fungal abundance, known to be more efficient at attacking recalcitrant substrates than bacteria (Hieber & Gessner, 2002; Romaní, Fischer, Mille-Lindblom, & Tranvik, 2006). In fact, the close relation between vascular plant community and the entire detected microbial functional gene profile was reflected in the high percentage variation in microbial community that was explained by plant variables in contract to soil variables. On the contrary, nonvascular plant (e.g., moss and lichen) biomass and productivity were not correlated with microbial functional gene profiles, possibly because their short root systems could not reach deeper soil layers where the microbial samples were collected. These results echoed many studies (De Long et al., 2016; Demarco, Mack, & Bret-Harte, 2014; Jonasson, Michelsen, & Schmidt, 1999; Lipson & Monson, 1998; Suding et al., 2008) showing that permafrost thaw affects soil microbial communities through above- and belowground biotic interactions.

We observed greater abundances of genes for ammonification and ammonia oxidation in the two sites with greater thaw, especially in the moderately thawed site. As a few studies reported significant correlations between N cycling process rates and corresponding gene/enzyme abundance (Liu et al., 2015; Morales, Cosart, & Holben, 2010; Trivedi et al., 2016; Wang et al., 2015; Xue, Yuan, Xie, et al., 2016), the higher abundances of *ureC* and *amoA* genes might indicate faster N turnover in thawed soils. This supports the finding that thaw tended to increase plant N availability, as indicated by higher total canopy N in the moderate and extensively thawed sites (Schuur et al., 2007), which could be associated with faster C decomposition and an increased N limitation after more permafrost is thawed for a longer period of time (Jonasson et al., 1999). The relatively low denitrification gene abundance under moderate thaw signaled less mineral N loss through direct reduction, which was supported by the soil stable isotopic N content. When there was no difference in $\delta^{15}N$ input to soil from the plant (Schuur et al., 2007), the lower $\delta^{15}N$ in the moderately and extensively thawed sites compared with the minimally thawed site potentially indicated lower fractions of ecosystem N loss through ^{15}N-depleted forms (NO_3^-, N_2O, etc.) (Amundson et al., 2003). Considering the high abundance of N assimilation genes *nirA* and nitrate reductase at the moderate and extensive thaw, the mineralized N was likely utilized by both plants and microbes. Yet, further studies are needed to directly measure functional processes to confirm these discussions.

We consistently detected the lowest abundances of genes involved in anaerobic processes under moderate thaw, including those involved in methanogenesis (*mcrA*), N fixation (*nifH*), denitrification (*nirK*, *norB*, *nirS*, and *nosZ*), dissimilatory N reduction (*napA*), and sulfite reduction (*dsrA/B*). This indicated that functional potentials for anaerobic reactions were more suppressed here, compared with minimally and extensively thawed sites. As contradictory it may seem with reported observations that thaw-induced saturated soil mosaics promote anoxic microbial processes (Coolen & Orsi, 2015; Lipson et al., 2015; Mackelprang et al., 2011; Waldrop et al., 2010), the EML study site is located at a well-drained mild slope with short period of visible water bogs only at the Ex sites in early summer. Only when the full soil depth profile is considered, water logging impacts deep soils for different lengths of time at the three sites. Thus, such topologic and hydrologic conditions did not result in a detectable increase in soil water content among our sites from our single time-point sampling. Conversely, ground subsidence could facilitate oxygen diffusion into areas below water table and plant roots also transport oxygen to the rhizosphere and the surrounding bulk soil (Husson, 2013; Ponnamperuma, 1972). At moderate thaw, these processes may have more thoroughly supported aerobic decomposition. Although the extensively thawed site had a greater maximum depression depth and higher plant biomass than the minimal site, soils here may remain saturated for a longer period of time than the other two sites. As thaw continues at EML, we may observe more severe water saturation and, subsequently, decreased oxidative potentials.

Notably, the explained variation in microbial functional potentials by the available plant and soil variables was low, probably because these measured environmental variables represent the conditions at the time of sampling rather than those spanning the sites' histories, which deterministically shape the microbial communities. Low temperatures in permafrost regions tend to preserve a large diversity of historical seed banks (Steven, Léveillé, Pollard, & Whyte, 2006; Willerslev et al., 2004) or dormant microbes (Lennon & Jones, 2011), that can be captured by DNA-based metagenomic techniques. In addition, stochastic processes (Stegen, Lin, Konopka, & Fredrickson, 2012; Zhou et al., 2013, 2014) may contribute to the diversity and succession of microbial communities, leading to the existence of rare and opportunistic species, which were captured by the closed-format, highly sensitive microarray (Zhou et al., 2015).

In summary, by analyzing the abundances of up to 40,000 functional genes probes in soils collected at EML across a gradient of naturally thawing permafrost, we found substantial differences in the profile of microbial functional potentials at the three stages of thaw. Genes involved in C and N cycling, as well as anaerobic processes, appeared to be most different at the moderately thawed site, potentially resulting from microbial interactions with plant communities, and ground subsidence upon thaw. Although the functional gene abundances were similar at minimally and extensively thawed sites, the later possessed a more divergent functional profile, which was likely related to a more heterogeneous microclimate after thaw intensified. Whether this divergent profile in Ex site will continue, or further developed thaw will serve to converge the communities to a new steady state, remains to be tested. Related studies on multiple functional process rates are still needed to reveal the mechanisms behind the complex responses of the microbial functional genes to long-term permafrost thaw.

CONFLICT OF INTEREST

The authors declare no conflict of interest.

REFERENCES

Abbott, B. W., Jones, J. B., Schuur, E. A. G., Chapin III, F. S., Bowden, W. B., Bret-Harte, M. S., ... Hollingsworth, T. N. (2016). Biomass offsets little or none of permafrost carbon release from soils, streams, and wildfire: An expert assessment. *Environmental Research Letters*, 11, 034014.

Amundson, R., Austin, A. T., Schuur, E. A. G., Yoo, K., Matzek, V., Kendall, C., ... Baisden, W. T. (2003). Global patterns of the isotopic composition of soil and plant nitrogen. *Global Biogeochemical Cycles*, 17, 1031.

Anderson, M. J. (2001). A new method for non-parametric multivariate analysis of variance. *Austral Ecology*, 26, 32–46.

Anderson, M. J., Ellingsen, K. E., & Mcardle, B. H. (2006). Multivariate dispersion as a measure of beta diversity. *Ecology Letters*, 9, 683–693.

Bais, H. P., Weir, T. L., Perry, L. G., Gilroy, S., & Vivanco, J. M. (2006). The role of root exudates in rhizosphere interactions with plants and other organisms. *Annual Review of Plant Biology*, 57, 233–266.

Chapin, F. S., Sturm, M., Serreze, M. C., McFadden, J. P., Key, J. R., Lloyd, A. H., ... Welker, J. M. (2005). Role of land-surface changes in arctic summer warming. *Science*, 310, 657–660.

Ciais, P., Sabine, C., Bala, G. Bopp, L., Brovkin, V., Canadell, J., ... Thornton, P. (2013). Carbon and other biogeochemical cycles. In T. F. Stocker, D. Qin, G.-K. Plattner, M. Tignor, S. K. Allen, J. Boschung, A. Nauels, Y. Xia, V. Bex & P. M. Midgley (Eds.), *Climate change 2013: The physical science basis. Contribution of working group I to the fifth assessment report of the intergovernmental panel on climate change* (pp. 470–471). Cambridge, UK and New York, NY, USA: Cambridge University Press.

Clarke, K. R. (1993). Non-parametric multivariate analyses of changes in community structure. *Australian Journal of Ecology*, 18, 117–143.

Coolen, M. J. L., & Orsi, W. D. (2015). The transcriptional response of microbial communities in thawing Alaskan permafrost soils. *Frontiers in Microbiology*, 6, 197.

De Long, J. R., Dorrepaal, E., Kardol, P., Nilsson, M.-C., Teuber, L. M., & Wardle, D. A. (2016). Understory plant functional groups and litter

species identity are stronger drivers of litter decomposition than warming along a boreal forest post-fire successional gradient. *Soil Biology and Biochemistry*, 98, 159–170.

De Mendiburu, F. (2014). Agricolae: statistical procedures for agricultural research. In: *R package version 1.2-0*.

Demarco, J., Mack, M. C., & Bret-Harte, M. S. (2014). Effects of arctic shrub expansion on biophysical vs. biogeochemical drivers of litter decomposition. *Ecology*, 95, 1861–1875.

Deng, J., Gu, Y., Zhang, J., Xue, K., Qin, Y., Yuan, M., . . . Zhou, J. (2015). Shifts of tundra bacterial and archaeal communities along a permafrost thaw gradient in Alaska. *Molecular Ecology*, 24, 222–234.

Euskirchen, E. S., Mcguire, A. D., Kicklighter, D. W., Zhuang, Q., Clein, J. S., Dargaville, R. J., . . . Smith, N. V. (2006). Importance of recent shifts in soil thermal dynamics on growing season length, productivity, and carbon sequestration in terrestrial high-latitude ecosystems. *Global Change Biology*, 12, 731–750.

Gavazov, K. S. (2010). Dynamics of alpine plant litter decomposition in a changing climate. *Plant and Soil*, 337, 19–32.

Grogan, P., Illeris, L., Michelsen, A., & Jonasson, S. (2001). Respiration of recently-fixed plant carbon dominates mid-winter ecosystem CO_2 production in sub-Arctic heath tundra. *Climatic Change*, 50, 129–142.

Hicks Pries, C. E., Schuur, EaG., & Crummer, K. G. (2012). Holocene carbon stocks and carbon accumulation rates altered in soils undergoing permafrost thaw. *Ecosystems*, 15, 162–173.

Hicks Pries, C. E., Schuur, E. A. G., & Crummer, K. G. (2013). Thawing permafrost increases old soil and autotrophic respiration in tundra: Partitioning ecosystem respiration using $\delta13C$ and $\Delta14C$. *Global Change Biology*, 19, 649–661.

Hieber, M., & Gessner, M. O. (2002). Contribution of stream detrivores, fungi, and bacteria to leaf breakdown based on biomass estimates. *Ecology*, 83, 1026–1038.

Hill, M. O. (1973). Diversity and evenness: A unifying notation and its consequences. *Ecology*, 54, 427–432.

Hobbie, S. E. (1996). Temperature and plant species control over litter decomposition in Alaskan tundra. *Ecological Monographs*, 66, 503–522.

Husson, O. (2013). Redox potential (Eh) and pH as drivers of soil/plant/microorganism systems: A transdisciplinary overview pointing to integrative opportunities for agronomy. *Plant and Soil*, 362, 389–417.

Jansson, J. K., & Taş, N. (2014). The microbial ecology of permafrost. *Nature Reviews Microbiology*, 12, 414–425.

Jonasson, S., Michelsen, A., & Schmidt, I. K. (1999). Coupling of nutrient cycling and carbon dynamics in the Arctic, integration of soil microbial and plant processes. *Applied Soil Ecology*, 11, 135–146.

Jorgenson, M. T., Racine, C. H., Walters, J. C., & Osterkamp, T. E. (2001). Permafrost degradation and ecological changes associated with a warming climate in central Alaska. *Climatic Change*, 48, 551–579.

Lawrence, D. M., & Slater, A. G. (2005). A projection of severe near-surface permafrost degradation during the 21st century. *Geophysical Research Letters*, 32, L24401.

Lee, H., Schuur, E. A. G., & Vogel, J. G. (2010). Soil CO_2 production in upland tundra where permafrost is thawing. *Journal of Geophysical Research: Biogeosciences*, 115, G01009.

Legendre, P., & Legendre, L. F. (2012). *Numerical ecology*. Amsterdam, the Netherlands: Elsevier.

Lennon, J. T., & Jones, S. E. (2011). Microbial seed banks: The ecological and evolutionary implications of dormancy. *Nature Reviews Microbiology*, 9, 119–130.

Lipson, D. A., & Monson, R. K. (1998). Plant-microbe competition for soil amino acids in the alpine tundra: Effects of freeze-thaw and dry-rewet events. *Oecologia*, 113, 406–414.

Lipson, D. A., Raab, T. K., Parker, M., Kelley, S. T., Brislawn, C. J., & Jansson, J. (2015). Changes in microbial communities along redox gradients in polygonized Arctic wet tundra soils. *Environmental Microbiology Reports*, 7, 649–657.

Liu, S., Wang, F., Xue, K., Sun, B., Zhang, Y., He, Z., . . . Yang, Y. (2015). The interactive effects of soil transplant into colder regions and cropping on soil microbiology and biogeochemistry. *Environmental Microbiology*, 17, 566–576.

Mackelprang, R., Saleska, S. R., Jacobsen, C. S., Jansson, J. K., & Taş, N. (2016). Permafrost meta-omics and climate change. *Annual Review of Earth and Planetary Sciences*, 44, 439–462.

Mackelprang, R., Waldrop, M. P., DeAngelis, K. M., David, M. M., Chavarria, K. L., Blazewicz, S. J., . . . Jansson, J. K. (2011). Metagenomic analysis of a permafrost microbial community reveals a rapid response to thaw. *Nature*, 480, 368–371.

Martiny, J. B. H., Bohannan, B. J. M., Brown, J. H., Colwell, R. K., Fuhrman, J. A., Green, J. L., . . . Staley, J. T. (2006). Microbial biogeography: Putting microorganisms on the map. *Nature Reviews Microbiology*, 4, 102–112.

Morales, S. E., Cosart, T., & Holben, W. E. (2010). Bacterial gene abundances as indicators of greenhouse gas emission in soils. *ISME Journal*, 4, 799–808.

Natali, S. M., Schuur, E. A., Trucco, C., Hicks Pries, C. E., Crummer, K. G., & Baron Lopez, A. F. (2011). Effects of experimental warming of air, soil and permafrost on carbon balance in Alaskan tundra. *Global Change Biology*, 17, 1394–1407.

Oksanen, J., Blanchet, F. G., Kindt, R. Legendre, P., Minchin, P. R., O'Hara, R. B., . . . Wagner, H. (2013). vegan: Community ecology package.

Osterkamp, T. E. (2007). Characteristics of the recent warming of permafrost in Alaska. *Journal of Geophysical Research*, 112, F02S02.

Osterkamp, T. E., Jorgenson, M. T., Schuur, E. A. G., Shur, Y. L., Kanevskiy, M. Z., Vogel, J. G., & Tumskoy, V. E. (2009). Physical and ecological changes associated with warming permafrost and thermokarst in Interior Alaska. *Permafrost and Periglacial Processes*, 20, 235–256.

Osterkamp, T. E., & Romanovsky, V. E. (1999). Evidence for warming and thawing of discontinuous permafrost in Alaska. *Permafrost and Periglacial Processes*, 10, 17–37.

Penton, C. R., Yang, C., Wu, L., Wang, Q., Zhang, J., Liu, F., . . . Zhou, J. (2016). *nifH*-harboring bacterial community composition across an Alaskan permafrost thaw gradient. *Frontiers in Microbiology*, 7, 1894.

Ponnamperuma, F. N. (1972). The chemistry of submerged soils. *Advances in Agronomy*, 24, 29–96.

R Core Team (2014). *R: A language and environment for statistical computing*. Vienna, Austria: R Foundation for Statistical Computing.

Rivkina, E., Laurinavichius, K., Mcgrath, J., Tiedje, J., Shcherbakova, V., & Gilichinsky, D. (2004). Microbial life in permafrost. *Advances in Space Research*, 33, 1215–1221.

Romaní, A. M., Fischer, H., Mille-Lindblom, C., & Tranvik, L. J. (2006). Interactions of bacteria and fungi on decomposing litter: Differential extracellular enzyme activities. *Ecology*, 87, 2559–2569.

Romanovsky, V. E., Smith, S. L., & Christiansen, H. H. (2010). Permafrost thermal state in the polar Northern Hemisphere during the international polar year 2007–2009: A synthesis. *Permafrost and Periglacial Processes*, 21, 106–116.

Schuur, E. A. G., & Abbott, B. (2011). Climate change: High risk of permafrost thaw. *Nature*, 480, 32–33.

Schuur, E. A. G., Abbott, B. W., Bowden, W. B., Brovkin, V., Camill, P., Canadell, J. G., . . . Zimov, S. A. (2013). Expert assessment of vulnerability of permafrost carbon to climate change. *Climatic Change*, 119, 359–374.

Schuur, E. A. G., Bockheim, J., Canadell, J. G., Euskirchen, E., Field, C. B., Goryachkin, S. V., . . . Zimov, S. A. (2008). Vulnerability of permafrost carbon to climate change: Implications for the global carbon cycle. *BioScience*, 58, 701–714.

Schuur, E. A. G., Crummer, K. G., Vogel, J. G., & Mack, M. C. (2007). Plant species composition and productivity following permafrost thaw and thermokarst in Alaskan tundra. *Ecosystems*, 10, 280–292.

—WILEY—

Schuur, E. A. G., Mcguire, A. D., Schadel, C., Grosse, G., Harden, J. W., Hayes, D. J., ... Vonk, J. E. (2015). Climate change and the permafrost carbon feedback. *Nature, 520*, 171–179.

Schuur, E. A. G., Vogel, J. G., Crummer, K. G., Lee, H., Sickman, J. O., & Osterkamp, T. E. (2009). The effect of permafrost thaw on old carbon release and net carbon exchange from tundra. *Nature, 459*, 556–559.

Stegen, J. C., Lin, X., Konopka, A. E., & Fredrickson, J. K. (2012). Stochastic and deterministic assembly processes in subsurface microbial communities. *ISME Journal, 6*, 1653–1664.

Steven, B., Léveillé, R., Pollard, W., & Whyte, L. (2006). Microbial ecology and biodiversity in permafrost. *Extremophiles, 10*, 259–267.

Suding, K. N., Ashton, I. W., Bechtold, H., Bowman, W. D., Mobley, M. L., & Winkleman, R. (2008). Plant and microbe contribution to community resilience in a directionally changing environment. *Ecological Monographs, 78*, 313–329.

Tarnocai, C., Canadell, J. G., Schuur, E. A. G., Kuhry, P., Mazhitova, G., & Zimov, S. (2009). Soil organic carbon pools in the northern circumpolar permafrost region. *Global Biogeochemical Cycles, 23*, GB2023.

Taş, N., Prestat, E., Mcfarland, J. W., Wickland, K. P., Knight, R., Berhe, A. A., ... Jansson, J. K. (2014). Impact of fire on active layer and permafrost microbial communities and metagenomes in an upland Alaskan boreal forest. *ISME Journal, 8*, 1904–1919.

Trivedi, P., Delgado-Baquerizo, M., Trivedi, C., Hu, H., Anderson, I. C., Jeffries, T. C., ... Singh, B. K. (2016). Microbial regulation of the soil carbon cycle: Evidence from gene-enzyme relationships. *ISME Journal, 10*, 2593–2604.

Trucco, C., Schuur, E. A. G., Natali, S. M., Belshe, E. F., Bracho, R., & Vogel, J. G. (2012). Seven-year trends of CO_2 exchange in a tundra ecosystem affected by long-term permafrost thaw. *Journal of Geophysical Research: Biogeosciences, 117*, G02031.

Tu, Q., Yu, H., He, Z., Deng, Y., Wu, L., Van Nostrand, J. D., ... Zhou, J. (2014). GeoChip 4: A functional gene-array-based high-throughput environmental technology for microbial community analysis. *Molecular Ecology Resources, 14*, 914–928.

Van Der Heijden, M. G. A., Bardgett, R. D., & Van Straalen, N. M. (2008). The unseen majority: Soil microbes as drivers of plant diversity and productivity in terrestrial ecosystems. *Ecology Letters, 11*, 296–310.

Van Sickle, J. (1997). Using mean similarity dendrograms to evaluate classifications. *Journal of Agricultural, Biological, and Environmental Statistics, 2*, 370–388.

Vogel, J. G., Schuur, E. A. G., Trucco, C., & Lee, H. (2009). Response of CO_2 exchange in a tussock tundra ecosystem to permafrost thaw and thermokarst development. *Journal of Geophysical Research: Biogeosciences, 114*, G04018.

Waldrop, M. P., Wickland, K. P., White Iii, R., Berhe, A. A., Harden, J. W., & Romanovsky, V. E. (2010). Molecular investigations into a globally important carbon pool: Permafrost-protected carbon in Alaskan soils. *Global Change Biology, 16*, 2543–2554.

Wang, M., Liu, S., Wang, F., Sun, B., Zhou, J., & Yang, Y. (2015). Microbial responses to southward and northward Cambisol soil transplant. *MicrobiologyOpen, 4*, 931–940.

Willerslev, E., Hansen, A. J., Rønn, R., Brand, T. B., Barnes, I., Wiuf, C., ... Cooper, A. (2004). Long-term persistence of bacterial DNA. *Current Biology, 14*, R9–R10.

Xue, K., Yuan, M. M., Shi, Z. J., Qin, Y., Deng, Y., Cheng, L., ... Zhou, J. (2016). Tundra soil carbon is vulnerable to rapid microbial decomposition under climate warming. *Nature Climate Change, 6*, 595–600.

Xue, K., Yuan, M. M., Xie, J., Li, D., Qin, Y., Hale, L., ... Zhou, J. (2016). Annual removal of aboveground plant biomass alters soil microbial responses to warming. *mBio, 7*, e00976–16.

Zhou, J., Deng, Y., Zhang, P., Xue, K., Liang, Y., Van Nostrand, J. D., ... Arkin, A. P. (2014). Stochasticity, succession, and environmental perturbations in a fluidic ecosystem. *Proceedings of the National Academy of Sciences, 111*, E836–E845.

Zhou, J., He, Z., Yang, Y., Deng, Y., Tringe, S. G., & Alvarez-Cohen, L. (2015). High-throughput metagenomic technologies for complex microbial community analysis: Open and closed formats. *mBio, 6*, e02288–14.

Zhou, J., Liu, W., Deng, Y., Jiang, Y.-H., Xue, K., He, Z., ... Wang, A. (2013). Stochastic assembly leads to alternative communities with distinct functions in a bioreactor microbial community. *mBio, 4*, e00584–12.

SUPPORTING INFORMATION

Additional Supporting Information may be found online in the supporting information tab for this article.